

CONSTRUCTION OF A JOINT PEAK-INTERVAL HISTOGRAM USING HIGHER-ORDER CUMULANT-BASED INVERSE FILTERING

Sheau-Fang Lei and Roger P. Hamernik

Auditory Research Laboratory
Plattsburgh State University
101 Broad Street
Plattsburgh, New York 12901, USA

ABSTRACT

Conventional metrics used to quantify signals in noise/hearing research rely primarily on time-averaged energy and spectral analyses. Such metrics, while appropriate for Gaussian-distributed waveforms, are of limited value in the more complex sound environments encountered in industrial/military settings that have nonGaussian and nonstationary-distributed waveforms. Recent research has shown that metrics incorporating the temporal characteristics of a waveform are needed to evaluate hazardous acoustic environments for purposes of hearing conservation. The joint peak-interval histogram is a prospective candidate for use in such an application. This paper shows that the joint peak-interval histogram can be obtained from an estimation of the temporal pattern of a complex noise waveform by using higher-order cumulant-based inverse filtering.

1. INTRODUCTION

Conventional metrics, such as the sound pressure level (SPL), and narrow or broadband (weighted) spectral energies, are used to evaluate the potential of an acoustic noise environment to produce a noise-induced hearing loss (NIHL). Such metrics can adequately quantify a noise having a steady-state waveform such as a continuous Gaussian noise and can be used to estimate the hazard to hearing from prolonged exposure to such noise. However, there is abundant evidence in the literature [3][4][8] showing that nonGaussian, nonstationary types of noises having the same energy and spectra as a Gaussian noise but different temporal structures, produce different audiometric and histological effects on the auditory system. Thus, conventional metrics are not adequate for the assessment of hearing hazards from noise exposures whose waveforms have nonGaussian and nonstationary characteristics. Such noises occur in many industrial environments.

Experiments using animal models [4][11] have demonstrated quite clearly that a simple A-weighted equivalent energy [9] is not a sufficient measure of hazard associated with nonGaussian noise environments. A report by Patterson et al. [10] concludes that both the energy and the peak SPL of an impact exposure are important variables in determining trauma. Demographic data [15][16] show that nonGaussian noise exposures are more hazardous to hearing than are Gaussian noises of similar equivalent energy (L_{eq}). Our own recent animal studies [4] have shown that noises that have the same L_{eq} and the same spectra but that differ considerably in their

temporal structure produce very different hearing losses, which are distributed very differently across audiometric test frequencies. Histological data confirm this result. A similar result involving up to 30 dB differences was found by Dunn et al. [3] using a much different experimental paradigm. The role of temporal variables is further emphasized in recent studies using interrupted noise exposure paradigms [6].

Based upon some of these early data we formulated the working hypothesis that, for the same total energy and spectrum, a high kurtosis noise exposure is more hazardous to hearing than a Gaussian noise exposure, and that this effect is frequency dependent. The truth of this statement is demonstrated in the Lei et al. [8] paper in which kurtosis (statistic) metrics in both the time and frequency domains were shown both to rank order the level of hearing trauma and to reflect the frequency specificity of trauma. These results are a clear indication that, in addition to energy, temporal and peak variables are important determinants of hearing loss. Since the kurtosis statistics reflects the peak and temporal structure of a nonGaussian noise, an algorithm that would yield these metrics along with peak and interval histograms would be highly desirable elements of a hearing conservation noise measurement system.

The fact that both temporal and spectral variables are important is not surprising since the cochlea has evolved into an exquisitely sensitive transducer of nonstationary stochastic signals typified by speech and music. Results such as outlined above have led to efforts to develop additional metrics which incorporate the temporal information inherent in the waveform of a noise. The joint peak-interval histogram, which shows the cumulative distribution of the peak amplitude reflections and timing intervals of the nonGaussian fluctuations in a noise waveform, is a candidate metric for quantifying noise exposures. This metric, in conjunction with conventional energy-based metrics, may prove to be useful in the evaluation of a noise environment for the protection of hearing. Higher-order cumulant-based filtering can be used to deconvolve noise waveforms to obtain the requisite amplitude and timing information for the construction of this proposed metric.

Complex noises [7], which simulate the nonstationary and nonGaussian characteristics of realistic industrial/military noise environments, have been used as experimental stimuli in animal studies of NIHL. These stimuli were shown to exacerbate hearing loss when compared to spectrally-equivalent Gaussian noises of the same energy [8]. The complex noise consisted of a high-level primary impulsive sequence and multiple reflected components superimposed on

a continuous Gaussian background noise. Such a stimulus, $x(k)$, can be expressed as:

$$\begin{aligned} x(k) &= s(k-k_0) + \alpha_1 s(k-k_1) + \alpha_2 s(k-k_2) + \dots + n(k) \\ &= u(k) \otimes s(k) + n(k) \\ u(k) &= \delta(k-k_0) + \alpha_1 \delta(k-k_1) + \alpha_2 \delta(k-k_2) + \dots \end{aligned} \quad (1)$$

where \otimes represents the convolution operator; $\delta(k)$ is the unit kronecker delta sequence; $s(k)$ is a primary impulsive sequence; $n(k)$ is the additive Gaussian distributed noise, and $u(k)$ is a reflectivity sequence containing information on the amplitude reflections and time delays (α_i are the reflected amplitude factors, and k_i are time delays). These factors and delays are independent random variables which control the amplitude fluctuations resulting from multipath interference, nonstationary sources, or characteristics of the propagating medium. If α_i and k_i can simultaneously be estimated from the complex noise samples alone, then α_i and k_i can be used to construct the joint peak-interval histogram. The deconvolution operation then can be applied to extract the reflectivity sequence of the complex noise waveforms.

2. DECONVOLUTION USING HIGHER-ORDER CUMULANT-BASED INVERSE FILTERING

The deconvolution operation is shown in the block diagram of Figure 1. The input excitation, $w(k)$, is desired and can be

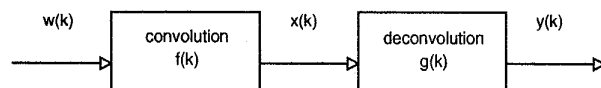


Figure 1. Block diagram of deconvolution operator to recover the input $w(k)$ from observed sequence $x(k)$ alone.

suitably estimated by measuring the response time series, $x(k)$, alone. A higher-order cumulant-based inverse filtering method [17] can be used to recover $w(k)$ when the information in the input excitation and convolution operation is unknown (i.e., "blind" deconvolution [2][5]). It has been shown that the output of any time-invariant linear operator with a white noise input results in a stationary random time series and that the magnitudes of the normalized cumulants of the output are less than or equal to the magnitude of the input excitation's normalized cumulant as shown in Equation (2) [1][2][12].

$$|K_y(p,q)| \leq |K_w(p,q)|, \quad K_y(p,q) = C_y(p)/C_y(q)^{p/q}; \quad \text{for } p > q \quad (2)$$

where $K_y(p,q)$ is the normalized cumulant of order (p,q) associated with output $y(k)$, and $C_y(q)$ is the q -order cumulant of y [14]. Based on this theorem, the algorithm for finding the inverse filter for the deconvolution can be initiated by selecting any integer values for p and q ; usually p is an even number and q is set equal to 2. The magnitude of the normalized cumulant, K_y , with respect to the linear operation between the input and output is then maximized. Since $f(k)$ is implicitly contained within the measured data, $x(k)$, the maximization must be made with respect to the deconvolution operator's impulse response, $g(k)$. If a higher-order cumulant-

based inverse filter is used to implement the deconvolution operator, the response normalized cumulant is dependent on the coefficients of this inverse filter, $g(k)$. This dependency will be highly nonlinear. A quasi-Newton method [13], used in nonlinear programming algorithms, can be used to find a functional relative maximum value of the function K_y . This method is similar to the steepest ascent algorithm but with a faster convergence to the maximum value of the objective function. A higher-order cumulant-based inverse filter is used in this paper because the implicit convolution operator is not necessarily of minimum phase. Also, higher-order cumulants are inherently immune to additive Gaussian noise.

The deconvolution model outlined above can be used to remove the effects of the primary impulsive sequence and to estimate the reflectivity sequence in a complex noise. An estimation of the reflectivity sequence, $u(k)$, extracted from samples, $x(k)$, of the waveform can provide temporal variation information on the nonGaussian component of a complex noise since the timing and the strength of the impulsive reflections can be obtained from $u(k)$. A higher-order cumulant-based inverse filtering is proposed for estimating the reflectivity sequence as shown in Figure 2. An inverse

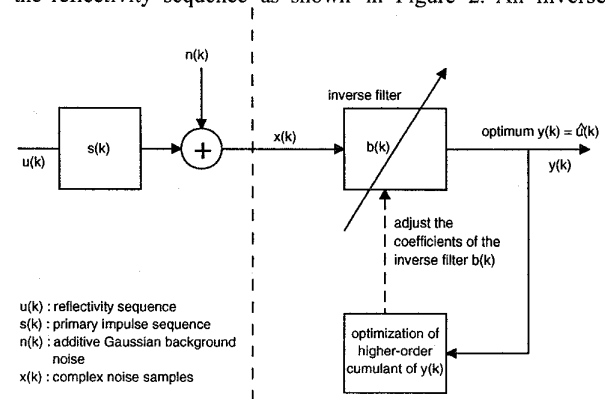


Figure 2. A higher-order cumulant-based inverse filter used to estimate the reflectivity sequence in a complex noise. The information of $u(k)$, $s(k)$, and $n(k)$ (shown on the left of the vertical dashed line) is implicitly contained in $x(k)$ and unknown to the deconvolution operator implemented by inverse filter $b(k)$.

filter, $b(k)$, acts as a deconvolution filter having as an input only the measured samples of $x(k)$. The fourth-order normalized cumulant, that is the kurtosis, shown in equation (3), is computed on the output sequence $y(k)$ of the inverse filter.

$$K_y(4,2) = \frac{E\{(y(k) - E\{y(k)\})^4\}}{(E\{(y(k) - E\{y(k)\})^2\})^2} - 3 \quad (3)$$

where $E\{ \cdot \}$ is the mean operator. The coefficients of $b(k)$ were obtained by maximizing the magnitude of the kurtosis values of the output sequence of this inverse filter. While we have used the fourth-order cumulant as an example to illustrate this estimate, the result can also be obtained by using other higher-order cumulant computations with the same

procedures. Since the higher-order cumulant values are highly nonlinear functions of the coefficients of $b(k)$, the coefficients of the inverse filter can be obtained by an iterative numerical optimization technique using a quasi-Newton method. The converged output sequence of the deconvolution will then be an optimum estimate of $u(k)$. The joint peak-interval histogram of the complex noise can then be constructed from the recovered temporal information that was hidden in $u(k)$.

3. SIMULATION RESULTS

Two complex noise waveforms having the same primary impulsive sequence were generated by computer simulation as shown in Figure 3(a). These two waveforms which have identical energy levels and spectra which is shown in Figure 3(b). Their temporal patterns, as seen in Figure 3(a), are different. Waveform I was generated by a reflectivity sequence whose amplitude reflections and timing delays were randomly distributed. In Waveform II the timing delays of the reflectivity sequence are periodic and the amplitude reflections have a random binary distribution. The reflectivity sequences of these two waveforms are shown in Figure 3(c). These two waveforms were processed by a fourth-order cumulant-based inverse filter to estimate their reflectivity sequence $u(k)$. This inverse filter was implemented by an FIR filter of order 14. The inverse filter coefficients were determined by maximizing the magnitude of the fourth-order cumulant of the output sequence, $y(k)$, as shown in Figure 2. The output sequences of these two waveforms are shown in Figure 3(d). These two sequences, resulting from

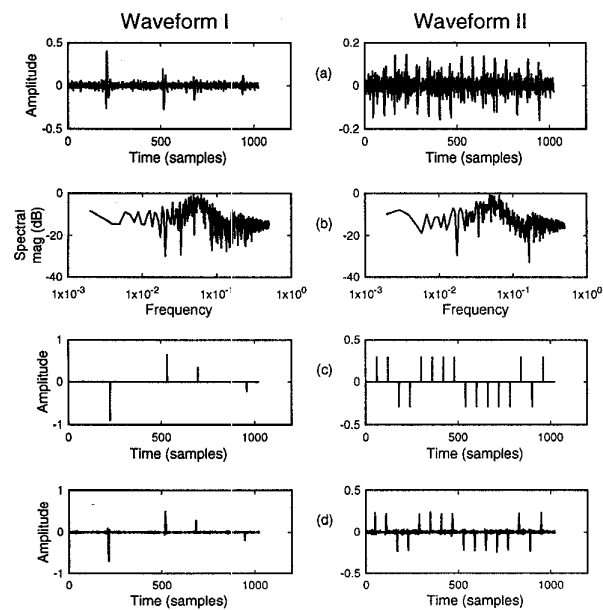


Figure 3. (a) Examples of two complex noise waveforms having different temporal structures. (b) Spectra of each of the temporal waveforms. (c) The reflectivity sequences of each of the temporal waveforms. (d) The reflectivity for each of the waveforms estimated from a fourth-order cumulant-based inverse filter analysis.

deconvolution by the inverse filter, are the optimum estimates of the reflectivity sequences. Comparison of Figures 3(c) and 3(d) indicate that the estimates provided by the inverse filtering are good estimates of the temporal patterns inherent in the original signals. The joint peak-interval histograms for the two waveforms shown in Figure 3(a) are presented in Figure 4. The amplitude and timing of each spike in the spike train sequences were recorded. The amplitude and temporal variable range was divided into 20 and 16 bins, respectively. The histograms were obtained from a cumulant-based inverse filtering analyses of 1,000 windows of the complex noise waveforms. The histograms show different contour shapes for each of the two waveforms. The shape of the histogram for Waveform I, shown in Figure 4(a), is relatively flat and uniform since the amplitude reflections and timing delays are uniformly and normally distributed. The shape of the histogram for Waveform II, shown in Figure 4(b), is periodically spiky and concentrated in the two binary value bins since the timing delays are periodic and the amplitude reflections are randomly binary distributed.

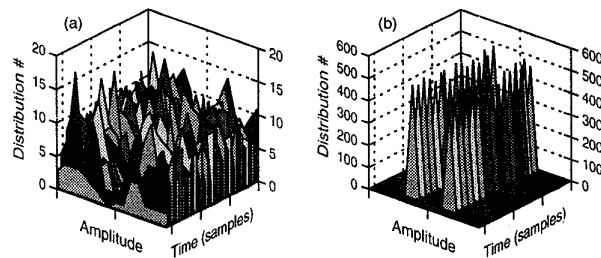


Figure 4. Joint peak-interval histograms of Waveforms I (a) and II (b). Amplitude range is from -1 to +1.

4. SUMMARY

This paper shows that a higher-order cumulant-based inverse filter can be used to estimate the reflectivity sequence within a complex noise waveform. The estimated reflective sequence can be used to differentiate between different temporal patterns which can then be quantified by the joint peak-interval histogram. All information on the temporal structure of a signal is lost in the conventional metrics that are based on energy and spectral computations. The joint peak-interval histogram along with kurtosis and energy-based metrics will contribute to the development of a measurement strategy that will allow us to order noise stimuli, having similar energy spectra, in terms of their potential for causing permanent changes to the auditory system. The primary focus of this paper was to present a method of obtaining the joint peak-interval histogram that could be incorporated into a noise analysis system. The utility of this histogram metric for assessing hearing hazards can ultimately only be determined from animal model experiments of the type described in Lei et al. [8].

5. REFERENCES

- [1] Cadzow, J.A. "Blind deconvolution via cumulant extrema". *IEEE signal processing Magazine*, 13(3):24-42, May 1996.

- [2] Cadzow, J.A. and Li, XingKang, "Blind deconvolution," *Digital Signal Processing Journal*, John Wiley, 5:(1):3-20, 1995.
- [3] Dunn, D.E., Davis, R.R., Merry, C.J., and Franks, J.R. "Hearing loss in the chinchilla from impact and continuous noise exposure". *Journal of the Acoustical Society of America*, 90(4):1979-1985, 1991.
- [4] Hamernik, R.P., Ahroon, W.A., Hsueh, K.D., Lei, S.-F., and Davis, R.I. "Audiometric and histological differences between the effects of continuous and impulsive noise exposures". *Journal of the Acoustical Society of America*, 93(4):2088-2095, 1993.
- [5] Haykin, S. editor. *Blind Deconvolution*. Englewood Cliffs, NJ, Prentice Hall, 1994.
- [6] Henderson, D., Campo, P., Subramaniam, M., and Fiorino, F. "Development of resistance to noise," in: *Noise-Induced Hearing Loss*, eds: A. Dancer, D. Henderson, R. Salvi, R.P. Hamernik, Mosby-Year Book, St. Louis, MO, p. 476-488. 1992.
- [7] Hsueh, K.D. and Hamernik, R.P. "A generalized approach to random noise synthesis: theory and computer simulation". *Journal of the Acoustical Society of America*, 87(3):1207-1217, 1990.
- [8] Lei, S.-F., Ahroon, W.A., and Hamernik, R.P. "The application of frequency and time domain kurtosis to the assessment of hazardous noise exposures". *Journal of the Acoustical Society of America*, 96(3):1435-1444, 1994.
- [9] Martin, A. "The equal energy concept applied to impulse noise," in: *The Effects of Noise on Hearing*, eds: D. Henderson, R.P. Hamernik, D.S. Dosanjh and J. Mills, Raven Press, NY. pp. 421-453. 1976.
- [10] Patterson, J.H., Lomba-Gautier, I.M., Curd, D.L., and Hamernik, R.P. "The role of peak pressure in determining the auditory hazard of impulse noise". USAARL Report 86-7.
- [11] Roberto, M., Hamernik, R.P., Salvi, R., Henderson, D., Milone, R.. "Impact noise and the equal energy hypothesis". *Journal of the Acoustical Society of America*, 77(4):1514-1520, 1985.
- [12] Shalvi, O. and Weinstein, E. "New criteria for blind deconvolution of nonminimum phase systems". *IEEE Transactions on Information Theory*, 36(2):312-321, March, 1990.
- [13] Shanno, D.F. "Conditioning of Quasi-Newton Methods for Function Mimimization". *Mathematics of Computing*, 24:647-656, 1970.
- [14] Stuart, A. and Ord, J.K. *Kendall's Advanced Theory of Statistics, Vol I, Distribution theory*. John Wiley, NY. 1994.
- [15] Taylor, W., Lempert, B., Pelmeur, P., Hemstock, I., and Kershaw, J. "Noise levels and hearing thresholds in the drop forging industry". *Journal of the Acoustical Society of America*, 76(3):807-819, 1984.
- [16] Theyry, L. and Meyer-Bisch, C. "Hearing loss due to partly impulsive industrial noise exposure at levels between 87 and 90 dB". *Journal of the Acoustical Society of America*, 84(2):651-659, 1988.
- [17] Tugnait, J.K. "Estimation of linear parametric models using inverse filter criteria and higher order statistics". *IEEE Transactions on Signal Processing*, 41:3196-3199, Nov. 1993.